The *Ab initio* Study and NBO Analysis of the Solvent Dielectric Constant Effects on the Structural Stability of the fMet-tRNA

M. Noei[a]* , H.Mossalayi[a] , H.Aghaee [b] , F.Naderi [c] ,F.Mollaamin[d]

[a]*Department of Chemistry, Mahshahr Branch , Islamic Azad University, Mahshahr, Iran*
[b]*Department of Chemistry ,Science and Research Branch, Islamic Azad University, Tehran Iran*
[c]*Department of Chemistry ,Shahre Qods Branch, Islamic Azad University, Tehran Iran*
[d]*Department of Chemistry, Qom Branch , Islamic Azad University, Qom, Iran*

_____

ABSTRACT

Formyl-methionine is always the first amino acid of polypeptide chain in prokaryote systems, although frequently it is removed after translation .In this case we studied about amino acid linkage to the proper tRNA which this process is controlled by the amino-acyl-tRNA synthesis. Theoretical study of binding the amino acid (formyl-methionine) to tRNA has been performed using quantum computational Ab initio HF and density functional B3LYP method using 3-21G(d,p) basis set in the different solvents to calculate structural optimization and the major stabilizing orbital for the bond (fMet-tRNA) were calculated by natural bond orbital(NBO) methodology. By NBO analysis we observed an effective interaction between the O32 lone pair(LP)and sigma anti bonding orbital (σ *)of O29-C30.This suggests an electronic transference from oxygen LP to anti bonding orbital(hyper conjugation effect) . Finally, we employed the density functional theory (DFT) and Hartree-Fock (HF) to calculated NMR parameters.

Keyword: *Natural bond orbital(NBO), fMet-tRNA ,Hartree-fock(HF),Density functional theory(DFT), amino-acyl-tRNA,*
_____

INTRODUCTION

It is generally accepted that initiation of protein synthesis in Escherichia coli starts with formyl-methionine, directed by the codons AUG or GUG.Protein synthesis proceeds by transfer of the growing polypeptide chain from the tRNA bound to the ribosomal P site to the incoming aminoacyl-tRNA in the adjacent A site. After translocation of the ribosome in the 30 direction of

_____

the mRNA, by the action of elongation factor G, the A site again becomes empty and the next codon exposed so that a new aminoacyl-tRNA ternary complex can be selected [1].

Synthetic polynucleotide containing AUG And/or GUG codons as well as natural mRNA have been used extensively in order to elucidate the mechanism of initiation of protein synthesis [2]. In all these studies it has been assumed that binding of fMet-tRNA to ribosome's is the polynucleotide. in bacteria the start codon AUG is recognized by fMet-tRNA. This tRNA does not recognize internal AUG codons.

Initiation of protein biosynthesis requires the correct positioning of charged initiator tRNA, fMet-tRNA in the ribosomal P-site of the mRNA-programmed 70S ribosome's [3-7].

The   rapid development of molecular biology in recent years has been mirrored by the rapid development of computer hardware and software. This improvement leaded to the development of sophisticated computational techniques and a wide range   of computer simulations involving such methods among the areas It is well observed that fMet-tRNA is the pharmacological targets of many of the drugs that are   currently in clinical use or in advanced clinical trials. Therefore, the implication throughout this paper has been profound is the modeling of fMet-tRNA structure and function, the chemical behavior of fMet- tRNA within drug design and also understanding at a molecular level of the   role of solvents in biotechnological applications [8-9].we selected adenine of tRNA structure(first nucleotide in acceptor arm of tRNA structure) and then perform modeling of fMet-tRNA. (Fig 1)
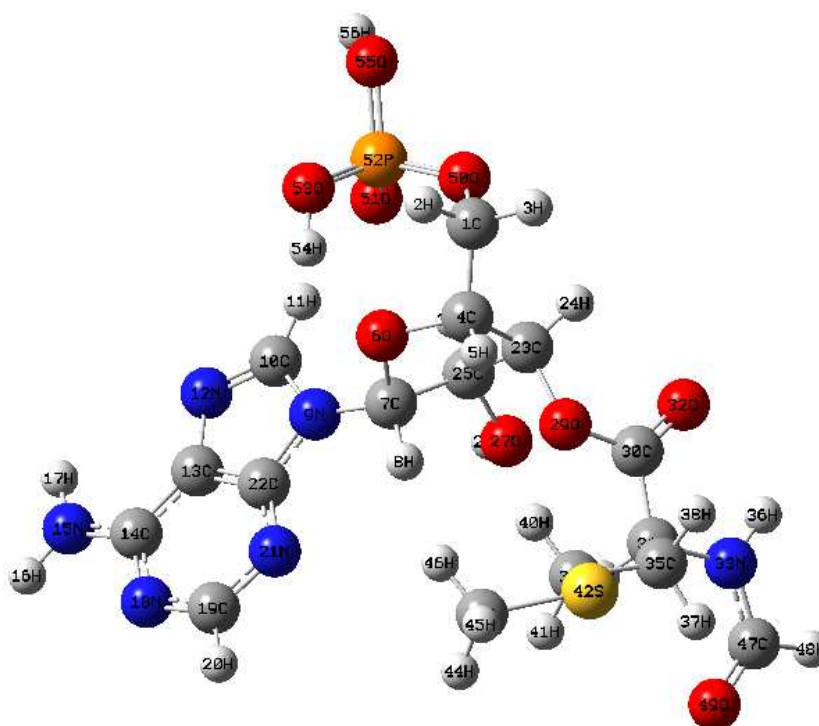

Fig .1: Structure of Adenine + fMet of fMet-tRNA

_____

Computational details

In our current study, extensive quantum mechanical calculations of structure of adenine + fMet (see Fig 1) and solvent effects on structure of adenine + fMet and calculations of NMR parameters and NBO calculation have been Performed on a Pentium-4 based system using GAUSSIAN 03 program .[10]

At first, we have modeled the structure of fMet-tRNA with Chem office package and then optimized at the B3LYP and HF levels of theory with 3-21G* basis set. After fully optimization of those structures , we have calculated NMR parameters and NBO analysis at the levels of HF/3-21G* and B3LYP/3-21G* theory and theoretically explored the solvent effects(GAS ,DMSO ,CHCL3,water) on structure of adenine + fMet All the relative energy values and NMR shielding parameters were calculated supposing gauge-included atomic orbital (GIAO) method [11]. Investigation on properties of fMet-tRNA is very important because this structure is initiation of protein biosynthesis.

This process involves sequential transformation of non-orthogonal atomic orbitals (AOs) to the sets of (natural atomic orbitals) NAOs, (natural hybrid orbitals) NHOs, and NBOs. Each of these localized basis sets is complete and describes the wave functions in the most economic method since electron density and other properties are described by the minimal amount of .filled orbitals in the most rapidly convergent way. Filled NBOs describe the hypothetical, strictly localized Lewis structure. The interactions between .filled and anti bonding (or Rydberg) orbitals represent the deviation of the molecule from the Lewis structure and can be used as the measure of delocalization. This non covalent bonding-anti bonding interaction can be quantitatively described in terms of the NBO approach that is expressed by means of the second-order perturbation interaction energy (E(2)) [12–15]. This energy represents the estimate of the off-diagonal NBO Fock matrix elements. It can be deduced from the second-order perturbation approach [16]

$$E^{(2)} = \Delta E_{ij} = q_i \frac{F(i,j)^2}{\varepsilon_j - \varepsilon_i} \tag{1}$$

Where qi is the donor orbital occupancy, εi, εj are diagonal elements (orbital energies) and F(i, j) is the off-diagonal NBO Fock matrix element.

RESULTS AND DISCUSSION

In this paper HF and DFT/B3LYP methods with 3-21G* basis set were Employed for investigating the structure optimization and energy minimization of fMet-tRNA (Fig1) have been summarized in Table 1.The HF and DFT energies are of particular interest because they provide results for interactions appearing in solvent medium considered in this letter, which are in accord with biological behavior of Adenine + fMet of fMet-tRNA. Furthermore, recent papers often tend to ask about the role of water solvent effect on the stability of Adenine + fMet of fMet-tRNA structure. The detailed results of relative energy values for Adenine + fMet of fMet-tRNA structure in gas , DMSO , CHCL3 and water solvents optimized at the HF and B3LYP levels of theory with 3-21G* basis set are summarized in Table (1) and Fig (2).

143

_____

Table1: Optimization Energy for each Method

3-21G*	E(kcal/mol)			
	Gas	**CHCl$_3$**	**DMSO**	**H$_2$O**
HF	-3738.1213366	-3738.1244432	-3738.1213031	-3738.1213011
B3LYP	-3755.0439622	-3755.0463986	-3755.0438037	-3755.0438020

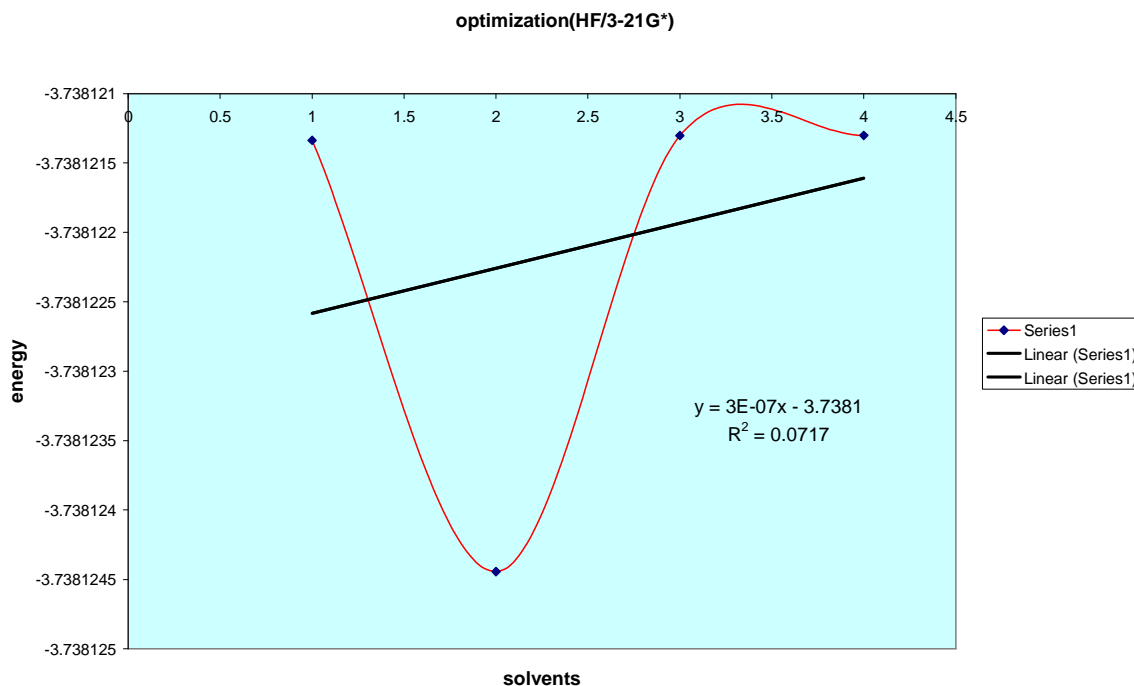**optimization(HF/3-21G*)**

$$y = 3E\text{-}07x - 3.7381$$
$$R^2 = 0.0717$$

Fig.2:optimization energy with 3-21G* basis set in different solvents, in value(x) axis, GAS(1), CHCl$_3$(2), DMSO(3) and H$_2$O(4)

In the NBO analysis, in order to compute the span of the valence space, each valence bonding NBO (σ_{AB}), must in turn, be paired with a corresponding valence anti bonding NBO (σ^*_{AB}): Namely, the Lewis σ-type (donor) NBO are complemented by the non-Lewis σ^*-type (acceptor) NBO that are formally empty in an idealized Lewis structure picture. Readily, the general transformation to NBO leads to orbitals that are unoccupied in the formal Lewis structure. As a result, the filled NBO of the natural Lewis structure are well adapted to describe covalency effects in molecules. Since the non-covalent delocalization effects are associated with $\sigma \rightarrow \sigma^*$ interactions between filled (donor) and unfilled (acceptor) orbitals, it is natural to describe them as being of donor–acceptor, charge transfer, or generalized "Lewis base-Lewis acid" type. The anti bonds represent unused valence-shell capacity and spanning portions of the atomic valence space that are formally unsaturated by covalent bond formation. Weak occupancies of the valence anti bonds signal irreducible departures from an idealized localized Lewis picture, i.e. true "delocalization effects". As a result, in the NBO analysis, the donor–acceptor (bond–anti bond) interactions are taken into consideration by examining all possible interactions between

144

_____

'filled' (donor) Lewis-type NBO and 'empty' (acceptor) non-Lewis NBO and then estimating their energies by second-order perturbation theory. These interactions (or energetic stabilizations) are referred to as 'delocalization' corrections to the zeroth-order natural Lewis structure.

The most important interaction between "filled" (donor) Lewis-type NBO and "empty" (acceptor) non-Lewis is reported in Table (2) , and Fig (3)the level of HF/3-21G* and B3LYP/3-21G* basis set at the DFT theory. we observed interaction between Donor NBO , the LP(1,2) of O29 , O32 and Acceptor NBO, the σ*(C30-O32) , π*(C30 - O32) , σ * (O29 - C30) of fMet-tRNA structure.

Table2:Second Order Perturbation Theory Analysis of Fock Matrix in NBO Basis
Threshold for printing: 0.50 (kcal/mol) HF/3-21G* method

Phase	Donor NBO (i)	Acceptor NBO (j)	E(2) (kcal/mol)
Gas	LP (1) O29	σ* C30 - O32	9.57
	LP (2) O29	π* C30 - O32	60.32
	LP (1) O32	σ* O29 - C30	0.58
	LP (2) O32	σ* O29 - C30	51.40
CHCL$_3$	LP (1) O29	σ* C30 - O32	9.62
	LP (2) O29	π* C30 - O32	60.72
	LP (1) O32	σ* O29 - C30	0.57
	LP (2) O32	σ* O29 - C30	51.15
DMSO	LP (1) O29	σ* C30 - O32	11.16
	LP (2) O29	π* C30 - O32	70.17
	LP (1) O32	σ* O29 - C30	1.64
	LP (2) O32	σ* O29 - C30	43.20
H2O	LP (1) O29	σ*C30 - O32	9.66
	LP (2) O29	π*C30 - O32	60.12
	LP (1) O32	σ *O29 - C30	0.58
	LP (2) O32	σ *O29 - C30	51.56

B3LYP/3-21G* method

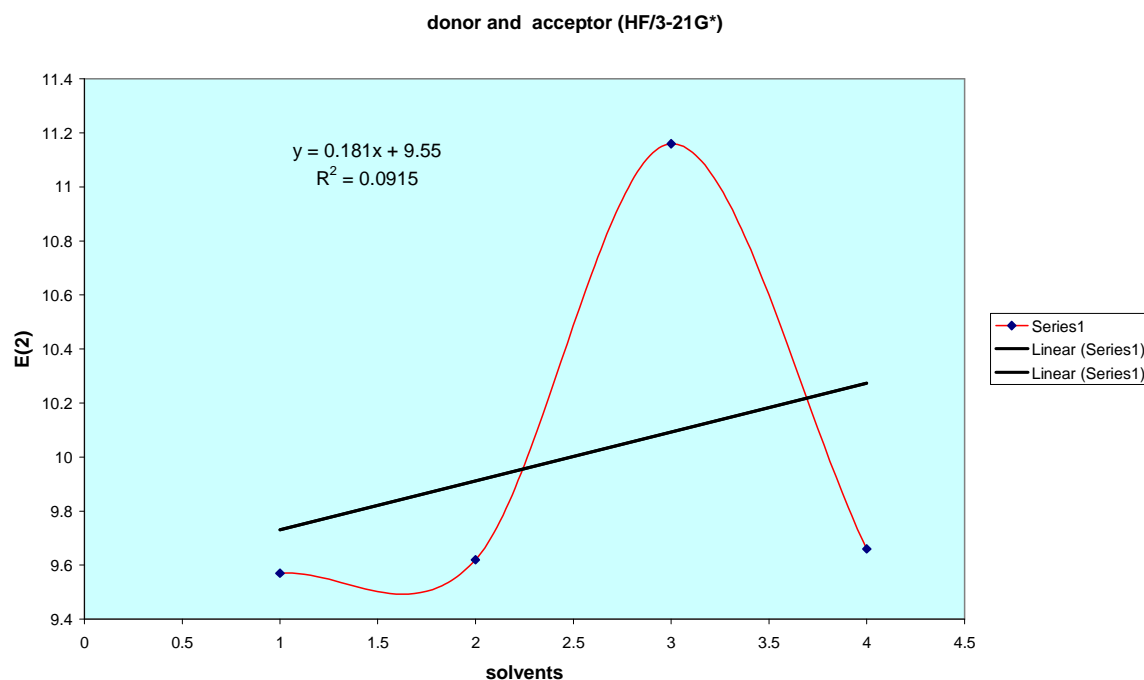| Phase	Donor NBO (i)	Acceptor NBO (j)	E(2) (kcal/mol)
Gas	LP (1) O29	σ* C30 - O32	7.25
	LP (2) O29	π* C30 - O32	55.35
	LP (1) O32	σ* O29 - C30	0.72
	LP (2) O32	σ* O29 - C30	37.09
CHCL3	LP (1) O29	σ* C30 - O32	7.28
	LP (2) O29	π* C30 - O32	55.66
	LP (1) O32	σ* O29 - C 30	0.71
	LP (2) O32	σ* O29 - C 30	36.98
DMSO	LP (1) O29	σ* C30 - O 32	8.34
	LP (2) O29	π* C30 - O32	50.45
	LP (1) O32	σ* O29 - C30	1.55
	LP (2) O32	σ* O29 - C30	37.09
H2O	LP (1) O29	σ* C30 - O 32	7.25
	LP (2) O29	π* C30 - O32	55.35
	LP (1) O32	σ* O29 - C 30	0.72
	LP (2) O32	σ* O29 - C 30	37.09

_____

donor and acceptor (HF/3-21G*)

Fig.3:donor[LP(1)O29] and acceptor[σ*C30-O29] energy [E(2)] with 3-21G* basis set in different solvents ,in value(x) axis ,GAS(1),CHCl₃(2),DMSO(3) and H₂O(4)

and then we reported the energy and hybrid for C30-O29 ,C30-O32 and C30=O32 bonding of fMet-tRNA Table (3), by same level.

Table3:Calculated natural hybrid orbitals (NHOs) and the polarization coefficient for each hybrid in the corresponding NBO (parentheses) for the selected fMet-tRNA using the selected methods.

Phase	Bond Hybrids	$C_{30}-O_{29}$		$C_{30}-O_{32}$		$C_{30}=O_{32}$	
		C_{30}	O_{29}	C_{30}	O_{32}	C_{30}	O_{32}
Gas	HF/3-21G*	$sp^{2.66}(0.5472)$	$sp^{1.93}(0.8370)$	$sp^{2.07}(0.5732)$	$sp^{1.26}(0.8194)$	$sp^{1.00}(0.5433)$	$sp^{1.00}(0.8396)$
	B3LYP/3-21G*	$sp^{2.64}(0.5602)$	$sp^{2.19}(0.8283)$	$sp^{2.12}(0.5811)$	$sp^{1.56}(0.8138)$	$sp^{99.99}(0.5660)$	$sp^{99.99}(0.8244)$
CHCL₃	HF/3-21G*	$sp^{2.64}(0.5484)$	$sp^{1.94}(0.8362)$	$sp^{2.07}(0.5735)$	$sp^{1.26}(0.8192)$	$sp^{1.00}(0.5448)$	$sp^{1.00}(0.8385)$
	B3LYP/ 3-21G*	$sp^{2.63}(0.5610)$	$sp^{2.20}(0.8278)$	$sp^{2.12}(0.5815)$	$sp^{1.57}(0.8136)$	$sp^{99.99}(0.5673)$	$sp^{99.99}(0.8235)$
DMSO	HF/3-21G*	$sp^{2.66}(0.5472)$	$sp^{1.93}(0.8370)$	$sp^{2.07}(0.5735)$	$sp^{1.26}(0.8192)$	$sp^{1.00}(0.5433)$	$sp^{1.00}(0.8396)$
	B3LYP/3-21G*	$sp^{2.66}(0.5472)$	$sp^{1.93}(0.8370)$	$sp^{2.07}(0.5732)$	$sp^{1.26}(0.8194)$	$sp^{99.99}(0.5660)$	$sp^{99.99}(0.8244)$
H2O	HF/3-21G*	$sp^{2.66}(0.5472)$	$sp^{1.93}(0.8370)$	$sp^{2.08}(0.5729)$	$sp^{1.26}(0.8196)$	$sp^{1.00}(0.5439)$	$sp^{1.00}(0.8392)$
	B3LYP/3-21G*	$sp^{2.64}(0.5602)$	$sp^{2.19}(0.8283)$	$sp^{2.12}(0.5811)$	$sp^{1.56}(0.8138)$	$sp^{99.99}(0.5660)$	$sp^{99.99}(0.8394$

_____

The natural population analysis (NPA) was evaluated in terms of natural atomic orbital occupancies [17,18]. Table 4 show the molecular charge distribution on the O29, C30 and O32 atoms in structure of fMet-tRNA . These partial charges distribution on the atoms   shows that the electrostatic repulsion or attraction between atoms can give a significant contribution to the intra- and intermolecular interaction.

Table4:Atomic charge distribution described in terms of natural population analysis (NPA) for the compounds studied

		Gas	CHCl₃	DMSO	H₂O
O29	HF/3-21G*	-0.63608	-0.63768	-0.63608	-0.714822
	B3LYP/3-21G*	-0.49088	-0.49162	-0.49088	-0.504795
C30	HF/3-21G*	0.94389	0.94185	0.94389	0.981579
	B3LYP/3-21G*	0.75659	0.75427	0.75659	0.732509
O32	HF/3-21G*	-0.64020	-0.63594	-0.64019	-0.621084
	B3LYP/3-21G*	-0.55198	-0.54844	-0.55197	-0.512211

Table (5)   and Fig (4) shows calculated natural orbital occupancy (number of electron, or ''natural population'' of the orbital). It is noted that for σO29 - C30 bond orbital, Decreased or increased occupancy of the localized σO29 - C30 orbital in the idealized Lewis structure, and their subsequent impact on molecular stability and geometry (bond lengths) are also related with the resulting p character of the corresponding O29 natural hybrid orbital (NHO) of σO29 - C30 bond orbital.

Table5: Occupancy and Energy (kcal/mol) for between O29 - C30 atoms (linkage area)

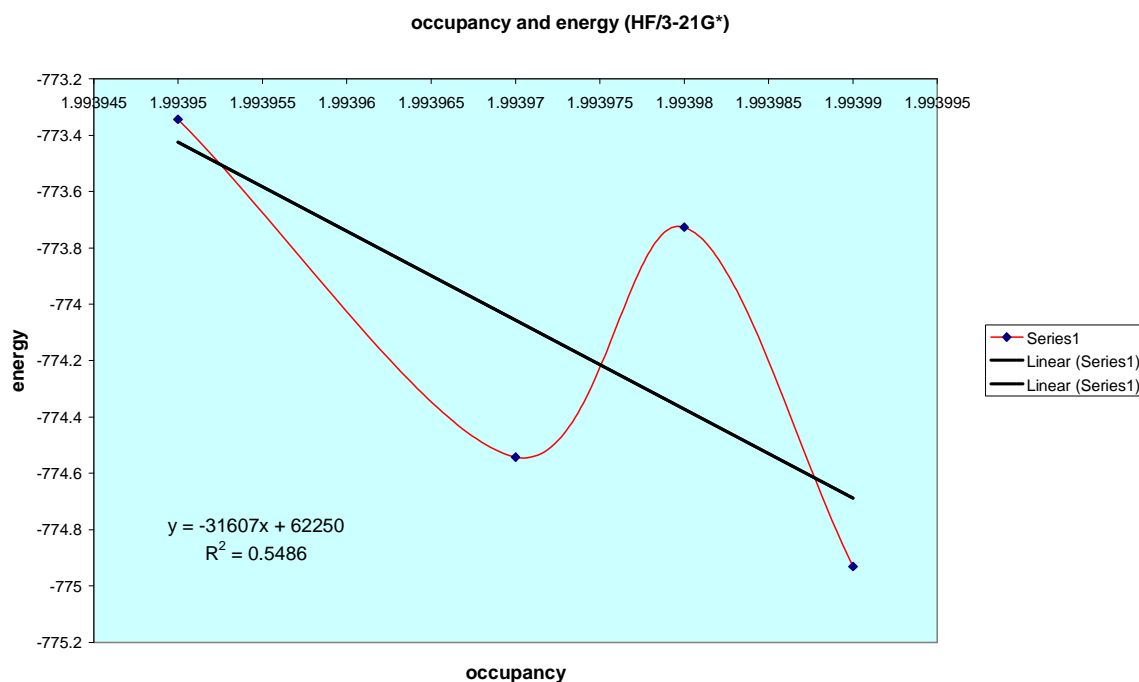| Phase	Method	NBO	Occupancy	Energy(kcal/mol)
Gas	HF/3-21G*	σ O29 - C30	1.99398	-773.7261
	B3LYP/3-21G*	σ O29 - C30	1.99305	-605.5910
CHCL₃	HF/3-21G*	σ O29 - C30	1.99399	-774.9309
	B3LYP/3-21G*	σ O29 - C30	1.99308	-606.6076
DMSO	HF/3-21G*	σ O29 - C30	1.99397	-773.5423
	B3LYP/3-21G*	σ O29 - C30	1.99305	-605.5910
H2O	HF/3-21G*	σ O29 - C30	1.99395	-773.3433
	B3LYP/3-21G*	σ O29 - C30	1.99305	-605.5910

_____

occupancy and energy (HF/3-21G*)

Fig.4: occupancy and energy for σO29-C30 with 3-21G* basis set in different solvents

Regarding most of the systems studied experimentally are in solution, the formulation of satisfactory theoretical models for solvated systems has been the object of continuously increasing interest. Therefore, *Ab initio* calculation of nuclear magnetic shielding has become an indispensable aid in the investigation of solvent effects on the structural stability and accurate theoretical NMR data of compounds [19-20].

As we know the effect of solvent molecules on fMet-tRNA plays an important role in the chemical behavior of fMet-tRNA we have already presented the results of our extensive studies of solvent induced effects on the NMR shielding of fMet-tRNA. Nuclear magnetic Resonance (NMR) is based on the quantum mechanical property of nuclei [21]. The chemical shielding refers to the phenomenon which associated with the secondary magnetic field created by the induced motions of the electrons that surrounding the nuclei when in the presence of an applied magnetic field. The energy of a magnetic moment μ, in a magnetic field, B, is as follow:

$$E = -\mu.(1-\sigma)B \qquad (2)$$

Where the shielding σ is the differential resonance shift due to the induced motion of the electrons [22]. In general, the electron distribution around a nucleus in a molecule is more spherically symmetric. Therefore, the size of electron current around the field, and hence the size of the shielding, will depend on the orientation of the molecule within the applied field B_0 [23].

148

_____

For chemical shielding (CS) tensor, which describes how the size of shielding varies with molecular orientation, we often use the following convention for the three principal components:

$$\sigma_{11} \leq \sigma_{22} \leq \sigma_{33} \qquad (3)$$

The three values of the shielding tensor are frequently expressed as the isotropic value (σ_{iso}), the anisotropy $(\Delta\sigma)$, and the asymmetry (η) There quantities are defined as follows [24]:

1)The isotropic value σ_{iso} :

$$\sigma_{iso} = \frac{1}{3}(\sigma_{11} + \sigma_{22} + \sigma_{33}) \qquad (4)$$

2) The anisotropy shielding $(\Delta\sigma)$:

$$\Delta\sigma = \sigma_{33} - \frac{1}{2}(\sigma_{11} + \sigma_{22}) \qquad (5)$$

and

3) The asymmetry parameter (η):

$$\eta = \frac{|\sigma_{22} - \sigma_{11}|}{|\sigma_{33} - \sigma_{iso}|} \qquad (6)$$

Instead of deriving $(\Delta\sigma_{ind})$ from the difference of the PCM- optimized shielding and the PCM shielding of the molecule held at the geometry optimized in vacuum, it can be obtained from the shielding calculated in vacuum for a molecule that is geometry-optimized in solution. [25]. Thus,

$$\Delta\sigma_{ind} = \sigma_{Vac}(R_{sol}) - \sigma_{Vac}(R_{ref}) \qquad (7)$$

Where $\sigma_{Vac}(R_{sol})$ is the value of the nuclear shielding in vacuum but with the solute geometry optimized in solution. $\sigma_{Vac}(R_{ref})$ are the corresponding parameters for calculation with reference solvent. In this case, we may suppose that optimization of solute molecule in solvent and then Performing shielding calculations is similar to shielding calculations in the isolated system [26].

Self-Consistent Reaction Field (SCRF) method is based on a continuum model with uniform dielectric constant (ε). The simplest SCRF model is the Onsager reaction field model . In this method, the solute occupies a fixed spherical cavity of radius a_0 within the solvent field. A dipole in the molecule will induce a dipole in the medium, and the electric field applied by the solvent dipole will in turn in interact with the molecular dipole leading to net stabilization.

The Gauge Including Atomic Orbital (GIAO) approach was used. The *Ab initio* GIAO calculations of NMR chemical shielding tensors were performed using the DFT and HF method. The chemical shielding tensors were calculated with the GAUSSIAN 03 program. The isotropic

_____

chemical shielding (σ_{iso}), asymmetry parameter (η) and anisotropy shielding $(\Delta\sigma)$ for O(29),O(32), C(30) atoms (Fig 1) have been summarized in Table(6). O(29),O(32)and C(30) atoms are very important in this structure ,because these atoms are agent bonding Between fMet and tRNA .

Table 6. NMR parameters(ppm) of O(29) and C (30) and O(32) in Adenine + fMet of fMet-tRNA structure in gas phase at the level of HF/3-21G* and B3LYP/3-21G* theory.

NMR parameters	GAS
HF/3-21G* O(29) σ_{iso}	221.0980
HF/3-21G* O(29) $\Delta\sigma$	229.6773
HF/3-21G* O(29) η	-1.7280
B3LYP/3-21G*O(29) σ_{iso}	137.0772
B3LYP/3-21G* O(29) $\Delta\sigma$	148.2147
B3LYP/3-21G* O(29) η	-0.7952
HF/3-21G* C(30) σ_{iso}	44.2825
HF/3-21G* C(30) $\Delta\sigma$	94.7091
HF/3-21G* C(30) η	14.5365
B3LYP/3-21G* C(30) σ_{iso}	36.1343
B3LYP/3-21G* C(30) $\Delta\sigma$	57.9762
B3LYP/3-21G* C(30) η	16.9674
HF/3-21G*O(32) σ_{iso}	-50.7765
HF/3-21G* O(32) $\Delta\sigma$	-52.6285
HF/3-21G* O(32) η	-1.6899
B3LYP/3-21G* O(32) σ_{iso}	-46.0160
B3LYP/3-21G* O(32) $\Delta\sigma$	-200.8172
B3LYP/3-21G* O(32) η	-0.5470

CONCLUSION

1-Optimization at the HF and DFT levels of theory provides a suitable computational model in terms of calculated NMR parameters and relative energies.
2-there was an increase in the relative stability of the interested structure through the improvement of basis set and including electron correlations , Hence, the most stable structure is perceived in the CHCL3 solution at the B3LYP/3-21G* level of theory.
3-we observed an increase in values of NMR chemical shielding around O29,O32 By increasing lone pair electrons contribution of oxygen (O29,O32) atoms in resonance interactions, Hence, O29 atom has the highest chemical shielding among the oxygen atoms.
4-we observed a decrease in the bond lengths of the O29-C30 of the structure by the increase of solvent dielectric constant.

_____

5- we observed an increase in the relative stability by increasing the LP Os(O29,O32) electrons contribution in the enhancement of π electron clouds.

6- we observed an increase in the energy of σO29-C30 by increasing occupancy of σO29-C30 in different solvents.

7- The largest σ_{iso} value of mentioned nuclei of Adenine + fMet of fMet-tRNA structure observed for O(29), whereas the smallest one belongs to O(32).It is interesting to note that the opposite trend have been observed for asymmetry parameters (η). This usual behavior may be readily understood in accord with biotechnological conceptions.

REFERENCES

[1] Ogle, J.M., and Ramakrishnan, V.(**2005**). *Annu. Rev. Biochem.* 74, 129-177.

[2] Grunberg-Manago, M.(**1977**). *Prog. Nuel. Acid Res. Mol.Biol.* 20,209-284.

[3] Gualerzi, C.O.and Pon, C.L.(**1990**). *Biochemistry* 29, 5881-5889.

[4] La Teana, A., Pon, C.L.and Gualerzi, C.O. (**1996**). .*J. Mol. Biol.*256,667-675.

[5] Gualerzi, C.O., Severini, M., Spurio, R.,La Teana, A. and Pon,C.L.(**1991**)..*J. Biol. Chem.* 266,16356-16362.

[6] Spurio, R., Severini, M., La Teana, A., Canonaco, M.A., Pawlik, R.T., Gualerzi, C.O. and Pon, C.L.(**1993**) in : The Translationa lApparatus: Structure, unction, Regulation, Evolution (Nierhaus, K.H., Franceschi, F., Subramanian, A.R., Erdmann, V.A. and Wittmann-Liebold, B.,Eds.), pp 241 252, Plenum Press, New York.

[7] Forster, C., Krait, C., Welfe, H.,Gualerzi, C.O. and Heinemann,U.(**1999**). *Acta Crystallogr.* D55,712-216.

[8] Agris.P.F;Guenther.R;Ingram.P.C; Basti. M.M.; Stuart.J.W;Sochacka.E.; Malkiewicz.A. RNA (**1997**). Unconventional structure of tRNA(Lys)SUU anticodon explains tRNA's role in bacterial and mammalian ribosomal frameshifting and primer selection by HIV,420-428.

[9] Isel.C;Ehresmann.C;Keith.G.;Ehresmann , B.; Marquet. R(**1995**)...*J. Mol. Biol.* 2247, 236-250

[10] Gaussian 98, Revision A.7,Frisch.M.J; Trucks. G.. W;Schlegel.H.B;Scuseria. G.E; Robb.M.A; Cheeseman. J. R;Z Zakrzewski. V.G; Montgomery.J. A; Stratmann;R.E; Burant J.C;Apprich. S; Millam.J. M; Daniels.A.D; Kudin.K.N; Strain.M.C; Farkas.O; Tomasi.J ;Barone.V; Cossi.M; Cammi.R; Mennucci.B; Pomelli. C; Adamoc; Clifford.S; Ochterski.J; Petersson. G.A; Ayala.P.Y; Cui.Q; Morokuma.K;Malick. D.K;Rabuck.A.D;Raghavachari.K; Foresman. J.B;Cioslowski. J; Ortiz.J.V; Baboul.A.G ; Stefanov.B.B; LIU.G;Liashenko. A; Piskorz.P; Komaromi.I; Gomperts.R; Martin.R.L;A; Fox. D. J; Keith. T; Al-laham.M.Peng. C. Y ; Nanayakkara .A; Gonzalez.C; Challacombe. M; Gill.P.M.W;Johnson. B; Chen. W; Wong. M.W;Andres.j. L; Gonzalez. C; Head-Gordon. M; Replogle. E.S and Pople.J. A(**1998**). Gaussian, Inc; Pittsburgh PA.

[11] Monajjemi.M;Chahkandi.B(**2005**). Study of HB different orientations of adenine – they mine base pairs; an ab iritio study Biochem Moscow.70, 366-376.

[12] A.E. Reed, F. Weinhold, *J. Chem. Phys.* 83 (**1985**) 1736.

[13] A.E. Reed, R.B. Weinstock, F. Weinhold, *J. Chem. Phys.* 83 (**1985**) 735.

[14] A.E. Reed, F. Weinhold, *J. Chem. Phys.* 78 (**1983**) 4066.

[15] J.P. Foster, F. Weinhold, *J. Am. Chem. Soc.* 102 (**1980**) 7211.

[16] J. Chocholousova, V. Vladimir Spirko, P. Hobza, *Phys. Chem. Chem. Phys.* 6 (**2004**) 37.

_____

[17] M. Haser, R. Ahlrichs, *J. Comput. Chem*. 10 (**1989**) 104.

[18] R. Ahlriches,M.Barr,M.Haser, H. Horn, C. Komel,*Chem.Phys. Lett*.162(**1989**) 65.

[19] Witanowski.M.;Sicinska.W;S.Biernat, Webbg.A(**1991**)..*J. Magn. J.Magn. Res*. 91, 289.

[20] Witanowski.M.;SICINSKA.W;Grabowski. Z.;Webb.G.A (**1990**).). *Mag. Res. Chem*. 28, 988.

[21] Benas. P.; Bec, G.; Keith, G.; Mrquet, R.; Ehresmann, C; Ehresmann, B. and Dumas, P.RNA (**2000**). The crystal structure of HIV reverse-transcription primer tRNA(Lys,3) shows a canonical anticodon loop 6 . 1347-1355

[22] Magdalena. P,Sadlej. Joanna (**1998**). *Chemical physics*. 234, 111-119.

[23] Melinda.A.J.D (**2003**). Solid state NMR spectroscopy; Principles and Applications, Cambridge press.

[24] Fazaeli.R;Monajjemi.M;Ataherian. F,Zare. K(**2002**). *J.M.Structure*(THEOCHEM).581,51-58

[25] Monajjemi. M; Heshmat. M;Aghaei. H;Ahmadi.R;Zare.k(**2007**). *Bull. Chem.Soc. Ethiop*. 21, 111-116.

[26] Lynden.Bell r. M; Rasaiah. J. C (**1997**). *J. Chem. Phys*. 107, 1981-1991.